

## Chapter 10 Spintronics

This is the final lecture of “Semiconductors.” I would like to close the lecture with a talk on semiconductor spintronics. Though the lecture time is limited, beginning with semi-classical spintronics, spin-orbit spintronics then finally we would like to consider the spin Hall effect and the topological insulators.

### 10.1 Classical treatment of spin transport

#### 10.1.1 What is spintronics?

So far we have seen transport phenomena in semiconductors from classical to quantum mechanical. An electron has a charge and simultaneously a spin, associated magnetic moment and angular momentum. Hence motion of an electron is associated not only with the charge but with the spin angular momentum. However, due to Kramers degeneracy, spin angular momentums cancel out each other and the microscopic transport of spin angular momentum does not appear in the net current. Since electrons are charge monopoles, electronics have made great progress by controlling their flow and accumulation, and semiconductors, which make this possible, have played a central role. However, now that the down-sizing, speeding up, and lowering of energy consumption are reaching their limits, spintronics is to use spin, which is the internal degree of freedom of electrons, for information storage and manipulation[1]. For a long time, magnetic disks and tapes, which are examples of spins frozen by the many-body effect, have been used for information storage. Giant magnetoresistance (GMR) devices, which utilize magnetic multilayers or spin-valve structure have been used for the readout of such information from 1990's. Since then, the word “spintronics” has been gradually used.

The reason why semiconductors were the center of electronics is, paradoxically, because they are insulators. It is most important that there are no electrons in an undisturbed crystalline state, and it is several times more difficult to cut off current in a metal with good control than to introduce conduction in an insulator, and in metal electronics. The role of metals in electronics is limited to wiring<sup>\*1</sup>. On the other hand in spintronics, there is no net spin in normal metals in equilibrium. They can be considered as “vacuum” for spins. In a sense, normal metals are semiconductors in spintronics, substances to be treated in semiconductor physics.

The above is by no means a play of words. In electronics, there is almost no electric field, that is, a slope of chemical potential in metals due to its short screening lengths. On the other hand, when an electric current is passed through an interface between a normal metal and a ferromagnet, the chemical potential is separated by spin. This is similar to the situation that in semiconductors under minority carrier injection in that different quasi Fermi levels are associated with electrons and holes. Also, even inside metals, the spin current causes gradients in chemical potentials that can be detected by external circuits. Therefore various physics we have seen in semiconductors may be observed as spintronics in normal metals in modified forms.

<sup>\*1</sup> However, the establishment of the concept of electronic circuits itself depends on the existence of a substance called metal. For the detail, see the lecture note of the present lecturer on electronics (in Japanese).

## 10.1.2 Two-current model

In the **two-current model** proposed by Nevil Mott, the net electric current by electrons is divided into the portions by up-spin ( $\uparrow$ ) and down-spin ( $\downarrow$ ) electrons. The model holds when the scattering time of spin flip is sufficiently longer than those by various mechanisms (Sec. 5.1.5) dominating conduction. The difference in the resistivities for  $\uparrow$  and  $\downarrow$  is due to the difference in parameters like density of states,  $k_F$ , etc. The total resistivity  $\rho$  is expressed by those for spin subband channels  $\rho_\uparrow, \rho_\downarrow$ , as  $1/\rho = 1/\rho_\uparrow + 1/\rho_\downarrow$ . In diffusive conductors, regardless of magnetic or non-magnetic, the spin diffusion length is generally longer than the mean free path ( $\lambda_F \gg l_F$ ), hence the two current model is considered to work well. On the other hand, in ballistic transport, particularly in the presence of strong spin-orbit interaction, the two-current model meets difficulty. In this section we treat classical transport with no or weak spin-orbit interaction. Hence the discussion is on the two-current model.

Assuming metallic conductors and the two-current model, we apply the Drude conductance to each spin-subband, which is given by  $\sigma_s = e^2 n_s \tau_s / m_s^*$  ( $s = \uparrow, \downarrow$ ). The net electric current density  $\mathbf{j}_c$  is given by  $\mathbf{j}_\uparrow + \mathbf{j}_\downarrow$  while the spin-polarized portion is given by the difference  $\mathbf{j}_{p\uparrow} = \mathbf{j}_\uparrow - \mathbf{j}_\downarrow$ . The polarization of **spin-polarized current** density is defined as

$$P_c = \frac{|\mathbf{j}_\uparrow - \mathbf{j}_\downarrow|}{|\mathbf{j}_\uparrow + \mathbf{j}_\downarrow|} = \frac{j_{p\uparrow(\downarrow)}}{j_c}. \quad (10.1)$$

Each component of the current is further divided into the drift term and the diffusion term as

$$\mathbf{j}_{ps} = \sigma_s \mathbf{E} - eD_s(-\nabla \delta n_s). \quad (10.2)$$

## 10.1.3 Spin-dependent electrochemical potential

Even when there is nonequilibrium between spin subbands by spin injection(or emission), providing that intra-subband scattering is sufficiently frequent and local equilibrium inside each spin band is kept, we can define local Fermi energy  $\epsilon_s$  and shift from the equilibrium  $\delta \epsilon_s$  for each spin-subband. For simplicity, a scalar  $\sigma_s$  is assumed for conductance tensor  $\sigma_s$ . We write the electrostatic potential as  $\phi$  ( $\mathbf{E} = -\nabla \phi$ ). The Einstein relation  $\sigma_s = e^2 N_s(E_F) D_s$  (this expression is low-temperature, metallic version of Eq. (5.13)),  $\delta n_s = N_s(E_F) \delta \epsilon_s$  gives the following.

$$\mathbf{j}_{ps} = -\frac{\sigma_s}{e} \left[ e \nabla \phi - \frac{D_s \nabla \delta n_s}{\sigma_s} \right] = \frac{\sigma_s}{e} [-e \nabla \phi + \nabla \delta \epsilon_s]. \quad (10.3)$$

In the two-current model, the local electrochemical potential for each spin can be defined as

$$\mu_s = -e\phi + \epsilon_s, \quad (10.4)$$

which leads to the expression of current density in each spin-subband

$$\mathbf{j}_{ps} = -\frac{\sigma_s}{-e} \nabla \mu_s. \quad (10.5)$$

Below we write electrochemical potential simply as “chemical potential.”

## 10.1.4 Spin current

There are several ways to define **spin current**, namely flow of spin angular momentum. A representative one is

$$\mathbf{j}^s(\mathbf{r}, t) = \frac{\hbar}{2(-e)} (\mathbf{j}_\uparrow - \mathbf{j}_\downarrow). \quad (10.6)$$

A spin current generally is a tensor formed by local spin density vector and flow vector. In the above for simplicity, we consider a spin current as a flow of  $z$ (direction of magnetization)-component of spin angular momentum. Also more generally, there is a type of spin current in which a flow of spin angular momentum is mediated by exchange interaction (e.g. by spin-wave).

With writing local spin angular momentum density as  $\mathbf{s}(\mathbf{r}, t)$ , and the  $z$  component as  $s_z$ , spin angular momentum conservation law is written by

$$\frac{\partial s_z}{\partial t} + \text{div} \mathbf{j}^s = 0. \quad (10.7)$$

In the presence of spin relaxation, we need to consider the relaxation term in the right hand side of Eq. (10.7). Within the relaxation time approximation, we can write

$$\frac{\partial s_z}{\partial t} + \text{div} \mathbf{j}^s = \frac{\partial s_z}{\partial t} + \frac{\hbar}{2(-e)} \nabla \cdot (\mathbf{j}_\uparrow - \mathbf{j}_\downarrow) = \frac{\hbar}{2} \left( \frac{\delta n_\uparrow}{\tau_\uparrow} - \frac{\delta n_\downarrow}{\tau_\downarrow} \right). \quad (10.8)$$

On the other hand, the charge ( $\rho$ ) conservation law is given by

$$\frac{\partial \rho}{\partial t} + \text{div} \mathbf{j} = \frac{\partial \rho}{\partial t} + \nabla \cdot (\mathbf{j}_\uparrow + \mathbf{j}_\downarrow) = 0. \quad (10.9)$$

In a steady state,  $\partial \rho / \partial t = \partial s_z / \partial t = 0$ . From the constraint that there should be no total spin flip in the whole system the relaxation times  $\tau_\uparrow$  and  $\tau_\downarrow$  should fulfill the detailed balance condition:

$$N_\uparrow \tau_\downarrow = N_\downarrow \tau_\uparrow, \quad (10.10)$$

where  $N_{\uparrow, \downarrow}$  are the spin-dependent density of states at the Fermi level. The above and Eqs. (10.8), (10.9) lead to

$$\nabla^2 (\sigma_\uparrow \mu_\uparrow + \sigma_\downarrow \mu_\downarrow) = 0, \quad (10.11a)$$

$$\nabla^2 (\mu_\uparrow - \mu_\downarrow) = \frac{1}{(\lambda_{\text{sf}}^{\text{F}})^2} (\mu_\uparrow - \mu_\downarrow). \quad (10.11b)$$

Averaged spin diffusion length  $\lambda_{\text{sf}}^{\text{F}}$  is defined from the Matthiessen's law as  $(\lambda_{\text{sf}}^{\text{F}})^{-2} = (\lambda_\uparrow^{\text{F}})^{-2} + (\lambda_\downarrow^{\text{F}})^{-2}$ , where  $\lambda_\uparrow^{\text{F}}$ ,  $\lambda_\downarrow^{\text{F}}$  are spin diffusion lengths for up and down spins respectively. Equation (10.11b) takes the form of diffusion equation, thus called **spin diffusion equation**.

## 10.2 Spin injection and relaxation

There are various methods of injecting spins into a paramagnetic material, similar to injecting minority carriers into a semiconductor by irradiating light or applying a forward bias to a pn junction. Here, in particular, spin injection from a ferromagnet to a paramagnetic material is described. As with minority carriers, spin injection occurs at the interface and spreads into the bulk and disappears (relaxes).

Let us consider an interface between a ferromagnet (FM) and a normal metal (NM) with a current  $j_c$  perpendicular to the interface. We write down the spin dependent local chemical potentials (Eq. (10.5)) for FM and NM regions in the following form:

$$\mu_s^{\text{M}} = a^{\text{M}} + b^{\text{M}} x \pm \frac{c^{\text{M}}}{\sigma_s^{\text{M}}} \exp\left(\frac{x}{\lambda_{\text{sf}}^{\text{M}}}\right) \pm \frac{d^{\text{M}}}{\sigma_s^{\text{M}}} \exp\left(-\frac{x}{\lambda_{\text{sf}}^{\text{M}}}\right), \quad (10.12)$$

where M is F(ferromagnet) or N(normal metal).  $x$ -axis is taken to be perpendicular to the interface in the direction to the normal metal, and the origin is taken at the interface. In the double sign  $\pm$ ,  $+$  corresponds to  $\uparrow$ ,  $-$  does  $\downarrow$ . The sum of the first two terms in the r.h.s. is written as  $\mu_0$ , which does not depend on spin. The function form of the third and the fourth terms comes from the fact that the spin-dependent parts should obey the diffusion equation (10.11). It is straightforward to confirm that the expression in Eq. (10.12) satisfies Eq. (10.11).

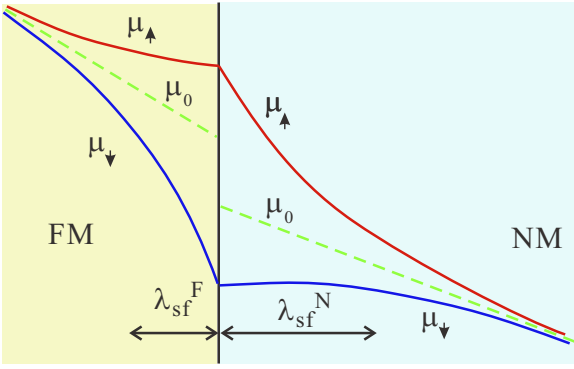


**Fig. 10.1** Sketch of spatial variation of spin-dependent chemical potential at an FM-NM interface, through which electrons flow from the FM side.

Coefficient  $a \sim d$  is determined as follows. Under the assumption of two-current model, the local chemical potential  $\mu_s$  for each spin subband must be continuous at the interface, i.e.  $\mu_s^F(-0) = \mu_s^N(+0)$ .  $\mu_0$  can be discontinuous at the interface for non-equilibrium states while in  $|x| \rightarrow \infty$  both in FM and NM the difference between  $\mu_\uparrow$  and  $\mu_\downarrow$  approaches zero. This means  $d^F = 0$  and  $c^N = 0$ . Also the sum of current densities in spin-subband should be the total current density  $j_c$ .

From the above, the density of states and the spin polarization in F  $P_F$ ,  $\mu_s^M$  is given by

$$\mu_s^F = \frac{(-e)j_c}{\sigma^F} x \mp \frac{(-e)j_c P_F \lambda_{sf}^N (1 - P_F^2) \sigma^F}{2\sigma_s^F \sigma^N \left[ 1 + (1 - P_F^2) \frac{\sigma^F \lambda_{sf}^N}{\sigma^N \lambda_{sf}^F} \right]} \exp\left(\frac{x}{\lambda_{sf}^F}\right), \quad (10.13a)$$

$$\mu_s^N = \frac{(-e)j_c}{\sigma^N} x + \frac{(-e)j_c P_F \lambda_{sf}^N}{\sigma^N \left[ 1 + (1 - P_F^2) \frac{\sigma^F \lambda_{sf}^N}{\sigma^N \lambda_{sf}^F} \right]} \left[ 1 \mp \exp\left(-\frac{x}{\lambda_{sf}^N}\right) \right]. \quad (10.13b)$$

In the complex symbol  $+$ ,  $-$  correspond to  $\uparrow$ ,  $\downarrow$  respectively. The origin of energy is taken to the chemical potential in equilibrium ( $j_c = 0$ ). A schematic diagram is given in Fig. 10.1(a).

## 10.2.1 Spin injection and detection

Semiconductors are appropriate for the control of electric conduction because they are insulators in their intrinsic states. Similarly, non-magnetic materials are appropriate for the control and operation of spin current. For that, however, spin injection into non-magnetic materials just like minority carrier injection in pn junctions, etc. In the configuration in

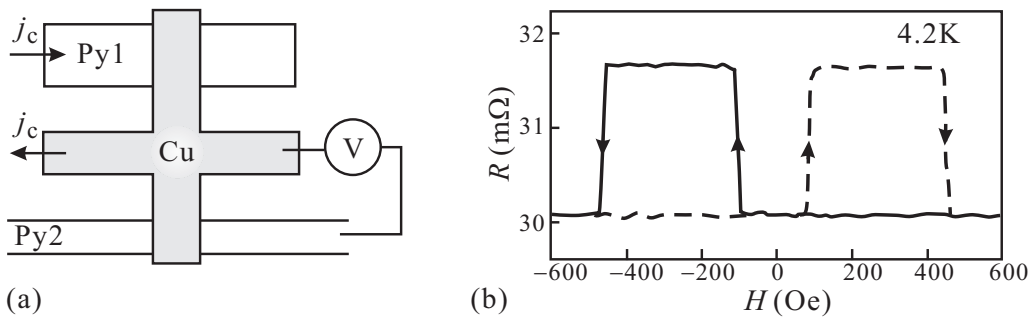


**Fig. 10.2** (a) Configuration of probes and circuit for non-local detection of spin injection. The electric current  $j_c$  goes through the center of the cross made of Cu to the left terminal while the spin current injected from Py1 reaches Py2, causes separation of  $\mu_\uparrow$  and  $\mu_\downarrow$  hence a step in  $\mu_0$  at the N-F (Cu-Py2) interface, which is detected as a voltage  $V$ . (b) Thus measured non-local resistance. The spin-valve like magnetoresistance comes from the difference in the coercive force between Py1 and Py2 due to the difference in the shape. The data are from [2].

Fig. 10.1, spin current and electric current are overlapped and the electric separation of the two effects is difficult. Therefore in many of experiments on spin injection, non-local configuration of electrodes is adopted.

An example is shown in Fig. 10.2. Current  $j_c$  through permalloy (alloy of Fe-Ni, Py)1 and the Cu sample causes separation of  $\mu_\uparrow$  and  $\mu_\downarrow$ , which means a spin accumulation at the interfaces. Though no electric current flows between Py2 and Cu, the spin diffusion occurs independently. The spin current thus also flows to Py2 and there causes difference in chemical potential, which is detected as a voltage. From Eq. (10.13) and the spin diffusion equation (10.11b), the detected voltage is given by

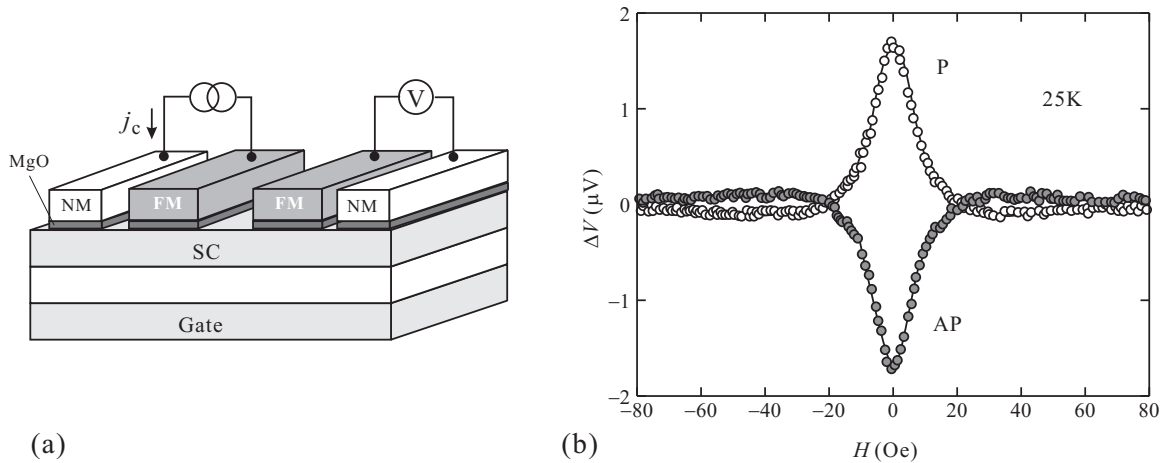
$$V = \pm \frac{1}{2} e j_c P_{Py}^2 \frac{\rho^{Py} \rho^{Cu}}{\rho^{Py} + \rho^{Cu}} \exp\left(-\frac{L}{\lambda_{sf}^{Cu}}\right). \quad (10.14)$$

Figure Fig. 10.2(b) shows the result of non-local measurement. Due to the difference in widths of Py1 and Py2, the coercive forces for the magnetic field along the strips are different, which results in the spin-valve like non-local magnetoresistance. The analysis of experimental results with various parameters by Eq. (10.14), material parameters like  $P_F$  and  $\lambda_{sf}$  can be obtained.

Figure Fig. 10.3(a) shows a schematic view of non-local four-terminal probe configuration, which is often adopted for the detection of spin injection into semiconductors. An electric current is applied between the left two electrodes including a ferromagnet, and the difference in the electrochemical potentials of the two electrodes also including a ferromagnet in the right is measured as a voltage. In such needle-shaped thin film electrodes, due to magnetic anisotropy from shape, the magnetic field is applied along the needles. On the other hand, a magnetic field perpendicular to the injected spins causes precession of spin magnetic moment (Appendix 10A). If the electron spins rotate in perfect coherence and the starting angle is also synchronized, the detected voltage oscillates reflecting the precession. In diffusion process, the distance of migration largely distributes and in real samples the region of injection has a finite width and the oscillation decays with the progress of precession. This is called Hanle effect.

If the problem is restricted to one dimensional spin diffusion along  $x$ -axis in a normal metal, spin dependence in  $\sigma_s$ ,  $D_s$  and  $\tau_s$  can be dropped in Sec. 10.1. In Eq. (10.2), since only the diffusion term is effective for non-local effect, the drift term is dropped. Applying the relaxation time approximation (10.8), we get the spin diffusion equation:

$$\frac{\partial s_z}{\partial t} = D \frac{\partial^2 s_z}{\partial x^2} - \frac{s_z}{\tau_{sf}}. \quad (10.15)$$



**Fig. 10.3** (a) Four terminal probe configuration for detection of spin injection into semiconductors (SCs) with non-local resistance. Current  $j_c$  between left pair of ferromagnet (FM) and normal metal (NM) causes spin current to the right, which is detected as the chemical potential difference (voltage). MgO for the potential barrier is used for spin-injection with high efficiency. (b) Hanle signal measured in a similar structure as in (a). The SC here is Si and the spin rotation is caused by the magnetic field perpendicular to the current plane. From Ref. [3].

This leads to the expression of Hanle signal:

$$\begin{aligned}\Delta V &= \pm \frac{j_e P_j^2}{e^2 N_{\text{SC}}} \int_0^\infty dt \varphi(t) \cos \omega t, \\ \varphi(t) &= \frac{1}{\sqrt{4\pi D t}} \exp\left(-\frac{d^2}{4Dt}\right) \exp\left(-\frac{t}{\tau_{\text{sf}}}\right),\end{aligned}\quad (10.16)$$

where  $d$  is the distance between the injection and detection electrodes,  $P_j$  is the spin polarization just below the injection electrode,  $\omega = g\mu_B B/\hbar$  is the Larmor frequency (Appendix 10A).

Figure Fig. 10.3(b) shows a Hanle signal measured in an experiment, in which spins were injected from an Fe electrode into Si. The signal can be fitted by (10.16). The fitting provides the parameters  $\lambda_{\text{sf}}$ , etc.

## 10.3 Spin-orbit interaction

Henceforth we go into semiconductor spintronics. Here ‘‘Semiconductor’’ refers to materials defined by the charge degrees of freedom that we have seen in the previous chapters. The spin-orbit interaction (SOI) has been already introduced when we had a look on k-p perturbation particularly for fcc-type semiconductors. In spintronics, the SOI is very important since it connects spin and orbital degree of freedoms. Below we see an example that the SOI becomes important even in the conduction bands through the mixing with the valence bands, in which the SOI is strong in intrinsic bulk states. More specifically, we consider two type of spin-orbit interactions in two-dimensional electron systems.

### 10.3.1 Spin-orbit splitting due to bulk and structural inversion asymmetries

In crystals when the lattice has the spatial inversion symmetry, the states of  $\mathbf{k}$  and  $-\mathbf{k}$  are degenerate. For example in the case of  $\uparrow$ -spin states,  $E(\mathbf{k}, \uparrow) = E(-\mathbf{k}, \uparrow)$ . The time-inversion operation causes  $-\mathbf{k} \rightarrow \mathbf{k}$  and simultaneously inversion in spin. When the crystals have time-inversion symmetry not having magnetism and the spatial inversion symmetry,  $E(\mathbf{k}, \uparrow) = E(\mathbf{k}, \downarrow)$ . In other words, in order for a system to have finite spin-splitting at finite  $\mathbf{k}$ , the system should have some inversion asymmetry.

In the primitive cell of zinc-blende type crystals, it is apparent that there is spatial inversion asymmetry along [111], which gives spin-splittings in energy dispersion due to the SOI. Such inversion asymmetries arising from crystal structures is called **bulk inversion asymmetry (BIA)**. SOIs caused by BIA is called **Dresselhaus spin-orbit interaction**. The Dresselhaus SOI is obtained from  $\mathbf{k} \cdot \mathbf{p}$  perturbation that takes BIA into account[4, 5]. BIA is some variance for  $\mathbf{k} \rightarrow -\mathbf{k}$ , and then the interaction term should be odd order in  $\mathbf{k}$ . In the caes of Dresselhaus interaction in three-dimensional systems is in 3rd order. The form of the Hamiltonian is

$$\mathcal{H}_{\text{DSO}}^{3\text{d}} = \gamma \hbar^2 [k_x(k_y^2 - k_z^2)\sigma_x + k_y(k_z^2 - k_x^2)\sigma_y + k_z(k_x^2 - k_y^2)\sigma_z], \quad (10.17)$$

where  $xyz$  is [100], [010], and [001]. When a two dimensional electron system (2DES) is formed on (001) surface, due to the averaging of kinetic freedom in  $z$ -direction ([001]), a  $k$ -linear term appears.

$$\begin{aligned}\mathcal{H}_{\text{DSO}}^{2\text{d}} &= \gamma \hbar^2 [k_x(k_y^2 - \langle k_z^2 \rangle)\sigma_x + k_y(\langle k_z^2 \rangle - k_x^2)\sigma_y] \\ &= \beta(k_y\sigma_y - k_x\sigma_x) + \gamma \hbar^2 (k_x k_y^2 \sigma_x - k_y k_x^2 \sigma_y).\end{aligned}\quad (10.18)$$

While the BIA is from the crystal structure, the inversion symmetry is broken by introducing some structures that break the periodicity like a hetro-interface. This is called **structure inversion asymmetry (SIA)**. The SOI introduced from the SIA at an interface is called **Rashba spin-orbit interaction** [6, 7]. The Rashba-type interaction Hamiltonian is written in the form:

$$\mathcal{H}_{\text{RSO}} = \alpha \boldsymbol{\sigma} \cdot (\mathbf{k} \times \mathbf{e}_z) = \alpha(k_y\sigma_x - k_x\sigma_y). \quad (10.19)$$

This comes from the expression Eq. (2.56). Here  $\nabla V$  (in (2.56)) is an electric-field like term perpendicular to the 2DES plane ( $z$ -direction)<sup>\*2</sup>. We need to be careful for “electric-field like term  $\nabla V$ .” Let us assume that this  $\nabla V/e$  is really an electric field for a while. Here,  $\nabla V$  is the total (including the one from the band discontinuity) force, which confines conduction electrons into the two-dimensional plane. The fact that the electrons are confined into the two-dimensional plane means that the averaged expectation value of  $\nabla V$  is zero due to the Ehrenfest theorem on the motion in  $z$ -direction, i.e.  $\langle \nabla V \rangle = 0$ [8]. Therefore, the Rashba interaction cannot be introduced from a real electric field  $\nabla V/e$ .

As seen in the  $k$ - $p$  approximation (Sec. 2.2.6-7), the SOI comes from the mixing of valence-band wavefunction into the conduction-band wavefunction at finite  $k$ . There, we introduced a potential  $V$  (Eq. (2.56)) common for conduction and valence bands. If there is a difference in their band discontinuities, we need to consider different  $V$ 's for them, and if  $\langle (\nabla V)_z \rangle = 0$  in the conduction band,  $(\nabla V)_z \neq 0$  in the valence band, then the Rashba interaction survives with that. Along the above line, we write the potentials in conduction and valence bands as  $V_c$  and  $V_v$  respectively and derive the expression for the SOI. Because  $\langle (\nabla V_c)_z \rangle = 0$ ,  $\nabla V$  term is replaced by  $\nabla V_v$ . In experiments, many phenomena characteristic to the Rashba SOI have been found, e.g. in a 2DES of a narrow gap semiconductor InGaAs. They are considered to arise from the valence band.

We consider a 2DES which only has  $k$ -linear terms in the Rashba SOI (10.19) and the Dresselhaus SOI (10.18). We take a plane wave with wavenumber  $\mathbf{k} = (k \cos \varphi, k \sin \varphi)$  as the orbital part to write the SOI Hamiltonian as follows.

$$\begin{aligned} \mathcal{H}_{\text{SO}} &= \alpha \begin{pmatrix} 0 & -i\hat{k}_x + \hat{k}_y \\ i\hat{k}_x + \hat{k}_y & 0 \end{pmatrix} + \beta \begin{pmatrix} 0 & -\hat{k}_x - i\hat{k}_y \\ -\hat{k}_x + i\hat{k}_y & 0 \end{pmatrix} \\ &= \alpha k \begin{pmatrix} 0 & ie^{-i\varphi} \\ -ie^{i\varphi} & 0 \end{pmatrix} - \beta k \begin{pmatrix} 0 & e^{i\varphi} \\ e^{-i\varphi} & 0 \end{pmatrix}. \end{aligned}$$

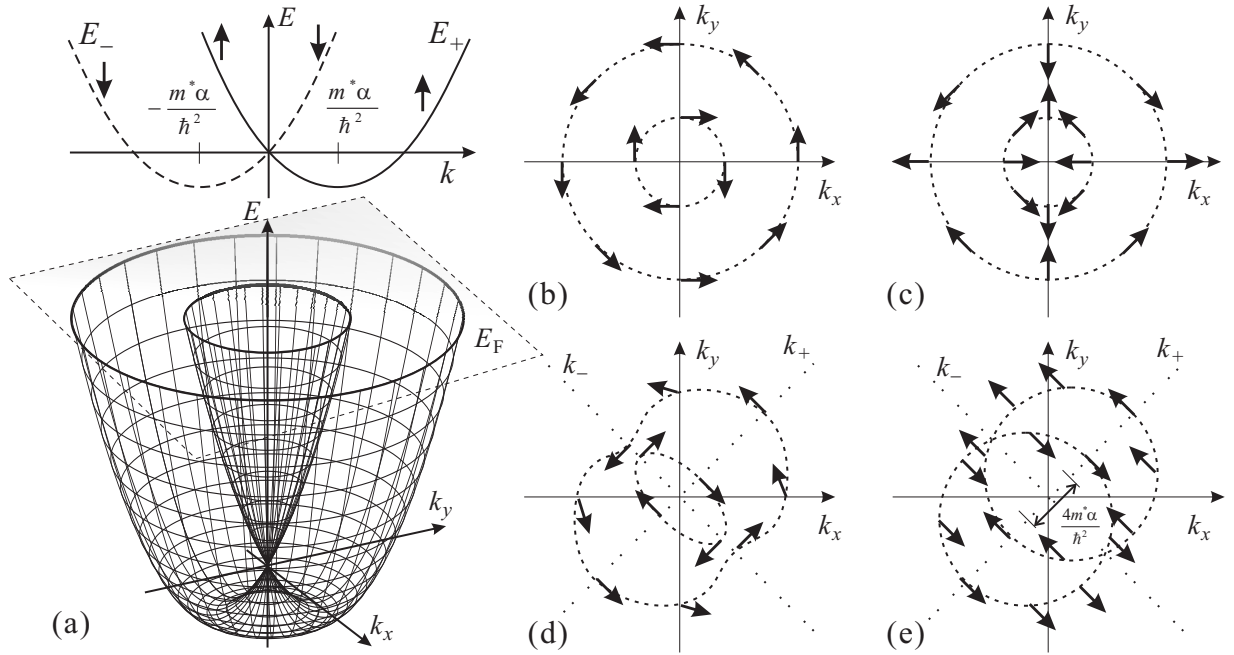


**Fig. 10.4** (a) Upper: Energy dispersion relation (10.20) in the presence of the Rashba SOI. The spin at  $+\pi/2$  is taken as “up.” Lower: Three dimensional wireframe expression of the energy dispersion on  $k_x - k_y$  plane. (b)~(e) are cross sections at  $E = E_F$ . (b) Two Fermi circles and the direction of effective field (spins) in the case of  $\beta = 0$  (Rashba model). (c) The same as (b) in the case of  $\alpha = 0$  (Dresselhaus model). (d)  $\alpha$  and  $\beta$  are finite, but  $\alpha \neq \beta$ . (e) The case of  $\alpha = \beta$ .

<sup>\*2</sup> From this expression, one often falls into the following incorrect explanation. – The existence of electric field means creation of charges both upper and lower sides of 2DES. From an electron running in 2DES those charges cause a loop current enclosing the 2DES. The loop current results in a magnetic field, which is nothing but the Rashba effective field. – For the reason why this is wrong, see the text.

In the case of  $\beta = 0$  (Rashba model), writing the spin part as  $t(1, e^{i\phi})/\sqrt{2}$ , we get  $\phi = \varphi \pm \pi/2$  from the condition of eigenfunction. Namely the wavevector and the spin are orthogonal. The eigenenergy  $E_{\pm}$  corresponding to  $\pm\pi/2$  are obtained in the effective mass approximation as

$$E_{\pm} = \frac{\hbar^2 k^2}{2m^*} \mp \alpha k = \frac{\hbar^2}{2m^*} \left( k \mp \frac{m^* \alpha}{\hbar^2} \right)^2 - \frac{m^*}{2\hbar^2} \alpha^2. \quad (10.20)$$

Equation (10.20) indicates that the dispersion shifts in  $k$ -space depending on the direction of spin. The dispersion is described as two spin-dependent parabolas as drawn in Fig. 10.4(a), and in Fig. 10.4(b) in a three-dimensional view. If we cut the dispersion at  $E = E_F$ , two cocentric Fermi circles appear. The direction of spin on the Fermi circles indicated in Fig. 10.4(b) rotates inversely to each other. Similarly for  $\alpha = 0$ ,  $\phi = -\varphi$ ,  $-\varphi + \pi$  and the energy dispersion is in the same form as Eq. (10.20) but with replacing  $\alpha$  with  $\beta$ . However, a rotation of  $\mathbf{k}$  on the Fermi circles causes an inverse rotation of spin as sketched in Fig. 10.4(c).

Under the coexistence of  $\alpha$  and  $\beta$ , generally the spin and the dispersion show complicated forms as in Fig. 10.4(d). In the special case of  $\alpha = \beta$ , the plane wave and the spin are separated as  $\mathcal{H}_{\text{SO}} = \alpha(\hat{k}_x + \hat{k}_y)(\sigma_x - \sigma_y)$ . With rotating the wave-vector part and the spin part as  $k_{\pm} = \frac{k_y \pm k_x}{\sqrt{2}}$ ,  $\chi_{\pm} = \pm^t(1/\sqrt{2}, (i-1)/2)$ , the Hamiltonian is expressed as

$$\mathcal{H} = \frac{\hbar^2}{2m^*} (\hat{k}_+^2 + \hat{k}_-^2) - 2\alpha \hat{k}_+ \sigma'_z. \quad (10.21)$$

$\sigma'_z$  is a Pauli matrix on the basis of  $\chi_{\pm}$ . Since the wave-vectors and the spins are separated, once the eigenfunction of the spin part  $\chi_{\pm}$  is determined, the dispersion is ordinary parabola whose center shifts by  $\pm 2m^* \alpha / \hbar^2$  depending on  $\chi_+$ ,  $\chi_-$ . Therefore, as in Fig. 10.4(e), the centers of the spin-dependent two parabolas shift to each other. The two center-shifted Fermi circles have a partial overlap.

### 10.3.2 Spin-orbit interaction and SdH oscillation

In a 2DES where the Rashba interaction is strong and  $\beta$  can be ignored, two Fermi circles with different  $k_F$  exist as in Fig. 10.4(b). This leads to spin-dependent 2DES sheet density  $n_{s\sigma} = k_{F\sigma}^2 / (4\pi)$ . The SdH oscillation in such a system should have two different periods in  $1/B$  plot as in Eq. (9.14) resulting in the beating among the two frequencies. The difference in the size of the Fermi circles is proportional to  $\alpha$ , thus to  $\langle \nabla V_{vz} \rangle$ . Therefore the frequency of beating should change with applying the external electric field to cause the change in  $\langle V_v \rangle$ .

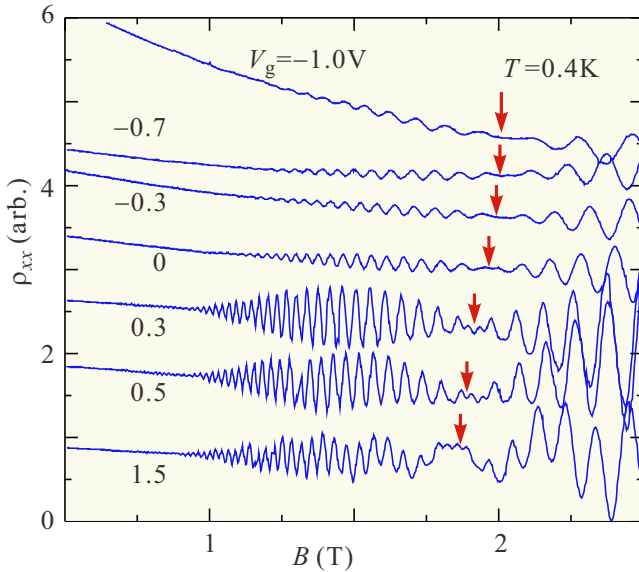


**Fig. 10.5** SdH oscillation observed in a 2DES at a quantum well of  $\text{In}_{0.53}\text{Ga}_{0.47}\text{As}$ . The parameter is the gate voltage  $V_g$  applied onto the surface of 2DES. The arrows indicate the position of nodes in the beats. From [9].

Figure 10.5(a) shows SdH oscillations measured in 2DES at a quantum well of (In,Ga)As grown on an InP substrate. Although there is a large lattice mismatch between InAs (narrow gap) and GaAs (relatively large gap), lattice matching is performed on the InP substrate by mixing crystals and setting the In composition to 0.53. In addition, heterojunctions can be formed by adding Al to the mixed crystal. A clear beat appears in the SdH oscillation, and the position of the node indicated by the arrow shifts due to the gate voltage, which is expected for the Rashba SOI.

## 10.4 Spin Hall effect and topological insulator

### 10.4.1 Spin Hall effect

When an electric field is applied to an electron system with SOI, a spin current is driven in the direction perpendicular to the field. This phenomenon is called spin Hall effect. Let  $J_{ij}$  be the spin current tensor with spin coordinate index  $i$ , flow coordinate index  $j$ . For the external electric field  $\mathbf{E}$ ,  $J_{ij}$  is written as

$$J_{ij} = \sigma_s \sum_k \epsilon_{ijk} E_k, \quad (10.22)$$

where  $\epsilon_{ijk}$  is the completely antisymmetric tensor indicating the mutual orthogonality of spin, flow vector of spin current and electric field.  $\sigma_s$  is called spin Hall conductance. The spin Hall effect arises from impurity scattering, or SOI from special orbital motion due to the band structure. The former is called extrinsic spin Hall effect while the latter is called intrinsic spin Hall effect.

Due to space limitation here I just introduce an example of experiment. Figure 10.6 shows an experiment, in which a spin accumulation at edges of an  $n$ -type GaAs sample is detected by the difference in chemical potentials of ferromagnetic electrodes. A clear spin signal which reverts with current reversal is detected (no signal for anti-parallel magnetization configuration). The signal is due to the spin Hall effect. From the temperature dependence, it is concluded that the origin is the extrinsic effect.

### 10.4.2 Anomalous velocity and spin Hall effect

Let us consider the motion of a wavepacket in a crystal. The wavepacket is expanded by Bloch functions and the effect of external force  $\mathbf{F} = -e\mathcal{E}$  from electric field  $\mathcal{E}$  on each Bloch component is examined. We introduce ‘‘Bloch

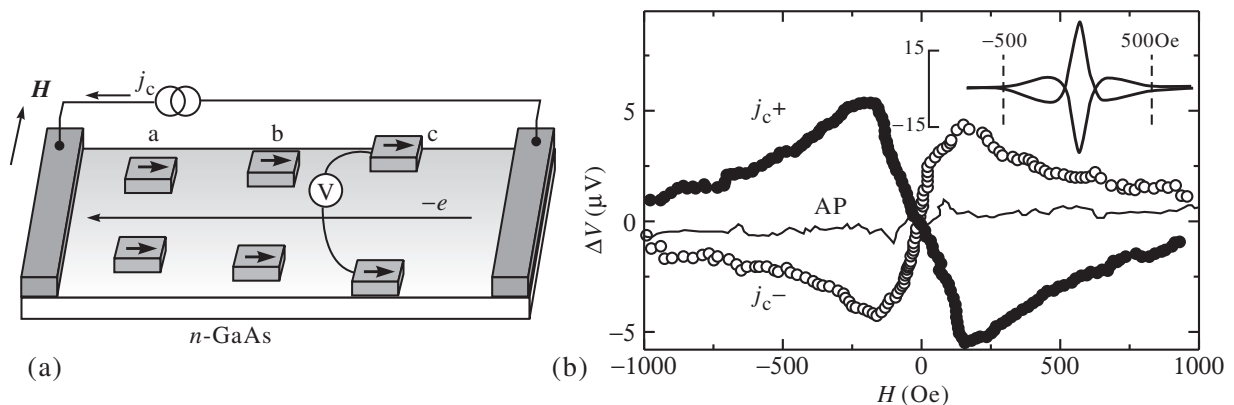


**Fig. 10.6** (a) Probe configuration of an  $n$ -type GaAs sample. Spin accumulation at the sample edges is detected by the Fe electrode pairs placed perpendicular to the current. (b) Spin Hall signal from electrodes at  $2 \mu\text{m}$  from the sample edges. The current density is  $5.7 \times 10^3 \text{ A/cm}^2$ . The solid and open circles are the results for reversed currents in parallel magnetization. The solid line is for anti-parallel magnetization. The inset shows the Hanle effect between the electrodes. The temperature is 30 K.

Hamiltonian"  $\mathcal{H}_B(\mathbf{k}) = e^{-i\mathbf{k}\cdot\mathbf{r}} \mathcal{H}_0 e^{i\mathbf{k}\cdot\mathbf{r}}$ , where  $\mathcal{H}_0$  is the crystal Hamiltonian, and the wave vector  $\mathbf{k}$  is treated as a parameter. And the eigenfunction is a lattice periodic function  $u_{n\mathbf{k}}(\mathbf{r})$ .

From the space of  $u_{n\mathbf{k}}(\mathbf{r})$ , a variation in  $\mathbf{k}$  can be viewed as that in the Hamiltonian. We have considered such situation in the introduction of Berry phase, in that the crystal wavenumber  $\mathbf{k}$  is taken as the set of parameters  $\mathbf{R}$  for adiabatic transition. Then the Berry connection and the Berry curvature in this case are

$$\mathbf{A}_n = i \left\langle u_{n\mathbf{k}} \left| \frac{\partial u_{n\mathbf{k}}}{\partial \mathbf{k}} \right. \right\rangle, \quad \mathbf{B}_n(\mathbf{k}) = i \left\langle \frac{\partial u_{n\mathbf{k}}}{\partial \mathbf{k}} \left| \times \right. \left| \frac{\partial u_{n\mathbf{k}}}{\partial \mathbf{k}} \right. \right\rangle, \quad (10.23)$$

respectively.

Let  $|n\mathbf{k}\rangle$  be a Bloch function, and we drop the band index  $n$  limiting the band to  $n$  (single band). We assume the quantities in Eq. (10.23) are not zero,  $\mathbf{k}$ -representation of the coordinate operator  $\hat{\mathbf{r}}$  is

$$\langle \mathbf{k} | \hat{\mathbf{r}} | \mathbf{k}' \rangle = (i\nabla_{\mathbf{k}} + \mathbf{A}) \delta(\mathbf{k} - \mathbf{k}'),$$

where  $\nabla_{\mathbf{k}} = \partial/\partial \mathbf{k}$ . This corresponds to that the dynamic momentum in a magnetic field is written as  $-i\hbar\nabla + e\mathbf{A}$  in the coordinate representation. Then we obtain

$$\langle \mathbf{k} | [\hat{x}, \hat{y}] | \mathbf{k}' \rangle = (i\nabla_{\mathbf{k}} \times \mathbf{A})_z \delta(\mathbf{k} - \mathbf{k}') = iB_z \delta(\mathbf{k} - \mathbf{k}').$$

From the Heisenberg equation  $d\hat{q}/dt = [\hat{q}, \mathcal{H}_0 - \mathbf{F} \cdot \hat{\mathbf{r}}]/i\hbar$ , we write the time evolution of operators  $\hat{x}, \hat{k}_x$  by  $\mathbf{F}$  as

$$\left\langle \mathbf{k} \left| \frac{d\hat{x}}{dt} \right| \mathbf{k}' \right\rangle = \left[ \frac{\partial E}{\partial k_x} - (\mathbf{F} \times \mathbf{B})_x \right] \frac{\delta(\mathbf{k} - \mathbf{k}')}{\hbar}, \quad \left\langle \mathbf{k} \left| \frac{d\hat{k}_x}{dt} \right| \mathbf{k} \right\rangle = F_x \frac{\delta(\mathbf{k} - \mathbf{k}')}{\hbar}.$$

Under the above conditions, a wavepacket  $f$  is expanded by Bloch functions as  $f = \sum_{\mathbf{k}} a_{\mathbf{k}} |\mathbf{k}\rangle$  ( $a_{\mathbf{k}} = \langle \mathbf{k} | f \rangle$ ). The time evolution of the averaged values of  $f$  in real and wavenumber spaces  $\mathbf{r}_0, \mathbf{k}_0$  are

$$\frac{d\mathbf{r}_0}{dt} = \mathbf{v} = \left\langle f \left| \frac{d\hat{\mathbf{r}}}{dt} \right| f \right\rangle = \sum_{\mathbf{k}} \frac{\langle f | \mathbf{k} \rangle}{\hbar} (\nabla_{\mathbf{k}} E - \mathbf{F} \times \mathbf{B}) \langle \mathbf{k} | f \rangle \approx \frac{1}{\hbar} (\nabla_{\mathbf{k}} E - \mathbf{F} \times \mathbf{B})|_{\mathbf{k}=\mathbf{k}_0}, \quad (10.24a)$$

$$d\mathbf{k}_0/dt = \mathbf{F}/\hbar, \quad (10.24b)$$

respectively. In (10.24a), the average over the wavepacket is replaced with the expectation value on  $\mathbf{k}$ . The second term in (10.24a) is the difference from the effective mass approximation due to the Berry curvature. This is called **anomalous velocity**.

When the Fermi level is within a band gap (i.e. the system is a band insulator) and the anomalous velocity exists, the Hall conductance is quantized as  $\sigma_{xy} = \nu e^2/h$  from the TKNN formula. However in ordinary situation with time-reversal symmetry, the Berry curvature  $\mathbf{B}$  is zero, no anomalous velocity exists, the Hall conductance disappears. As in the two current model the system is divided into  $\uparrow, \downarrow$  and we consider  $\sigma_{xy}^{\uparrow\downarrow}$  in each system. From the definition (10.6),  $j^s = (\hbar/(-2e))(\sigma_{xy}^{\uparrow} - \sigma_{xy}^{\downarrow})E$ . Therefore

$$\sigma_{xy}^s = \frac{\hbar}{-2e}(\sigma_{xy}^{\uparrow} - \sigma_{xy}^{\downarrow}) = \frac{-e}{4\pi}(\nu^{\uparrow} - \nu^{\downarrow}) = \frac{-e}{4\pi}\nu_s. \quad (10.25)$$

Here  $\nu^{\uparrow,\downarrow}$  is the Chern number for each spin subband and the difference between the two  $\nu_s$  is called spin Chern number. For the spin Chern number to be finite, there should be an effect that gives the same action as the magnetic field and the action should be reversed with spin reversal because in (10.25) the difference between the spin-subband is taken. Systems with a  $k$ -linear SOI just like Rashba model apparently fulfill the condition, which results in the appearance of the spin Hall effect.

### 10.4.3 Quantum spin Hall effect

The above discussion is for an insulator and we need to be careful about “electric curren of each spin” [10]. Even when the total net current is zero, current in each spin subband may be finite and in such a case, the Hall conductance is quantized by  $e^2/h$  in each subband. Let us consider the case the region  $y < 0$  in  $xy$ -plane is occupied with such a two-dimensional insulator. With Heaviside function  $\Theta(x)$ , the current components are  $j_x^\chi = \Theta(y)\sigma_{xy}^\chi E_y$ ,  $j_y^\chi = -\Theta(y)\sigma_{xy}^\chi E_x$ , where  $\chi$  is  $\uparrow$  or  $\downarrow$ . Then the charge conservation is written as

$$\frac{d\rho^\chi}{dt} + \nabla \cdot \mathbf{j}^\chi = \frac{d\rho^\chi}{dt} - \delta(y)\sigma_{xy}\chi E_x = \frac{d\rho^\chi}{dt} - \delta(y)\nu^\chi \frac{e^2}{h} E_x = 0.$$

Taking the difference between the two equations for  $\chi = \uparrow, \downarrow$ , and integrating on the entire space of the system, we get

$$\frac{dS_z}{dt} = L \frac{-e}{2\pi} \nu_s E_x,$$

where  $S_z$  is the  $z$ -component of total spin of the system,  $L$  is the length at the edge  $y = 0$ . The result tells that we need some anomaly at the edge to conserve  $S_z$ .

This leads to the idea of the edge states as in the quantum Hall effect, but in the present case there should be no net electric current. Then we consider two edge states (**helical edge states**) with opposite charge velocity and spin at the boundary. We write their dispersions as  $E_k^{\uparrow\downarrow} = \pm v(\delta k_x - eE_x t)$  ( $\uparrow$ :  $+$ ,  $\downarrow$ :  $-$ ,  $\delta k_x = k_x - k_F$ ). Because the variation in the number of particles in the unit time is  $\delta N_{\uparrow\downarrow} = \pm eE_x L/2\pi$

$$\frac{dS_z}{dt} = \frac{1}{2}(\delta N_\uparrow - \delta N_\downarrow) = L \frac{e}{2\pi} E_x.$$

With comparison of the two equations, from the condition  $dS_z/dt = 0$  in total, the number of helical edge states should be the spin Chern number.

Such an insulator is called quantum spin Hall insulator or **topological insulator**. Since spin Chern number is an integer, from Eq. (10.25), the spin Hall conductance of a topological insulator is quantized by  $e/4\pi$ .

### 10.4.4 Quantum well of a topological insulator

We will conclude this lecture by introducing an experiment that verified a topological insulator with quantum spin Hall effect for the first time. After this experiment, many topological insulators were discovered in a dozen years, and not only topological insulators but also Dilac semimetals and Weyl semimetals were found, and a wide range of topological materials such as magnetic ones were found. The research is now widely going on. In addition, the reason why we named

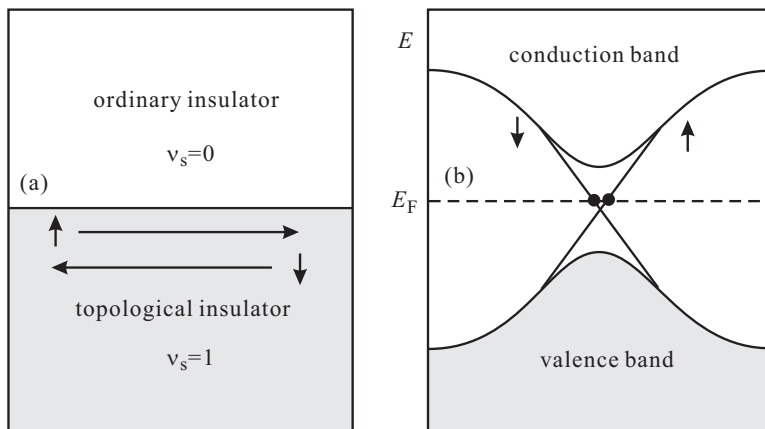


**Fig. 10.7** Concept of the topological insulator. (a) The region  $y < 0$  is a 2-dimensional topological insulator and the rest is a vacuum, which is an ordinary insulator. A pair of helical edge states exists at the boundary. The spin Chern number in the topological insulator is 1 corresponding to the nubner of edge states. (b) The energy dispersion diagram. The helical edge states have a linear dispersion relation[10].

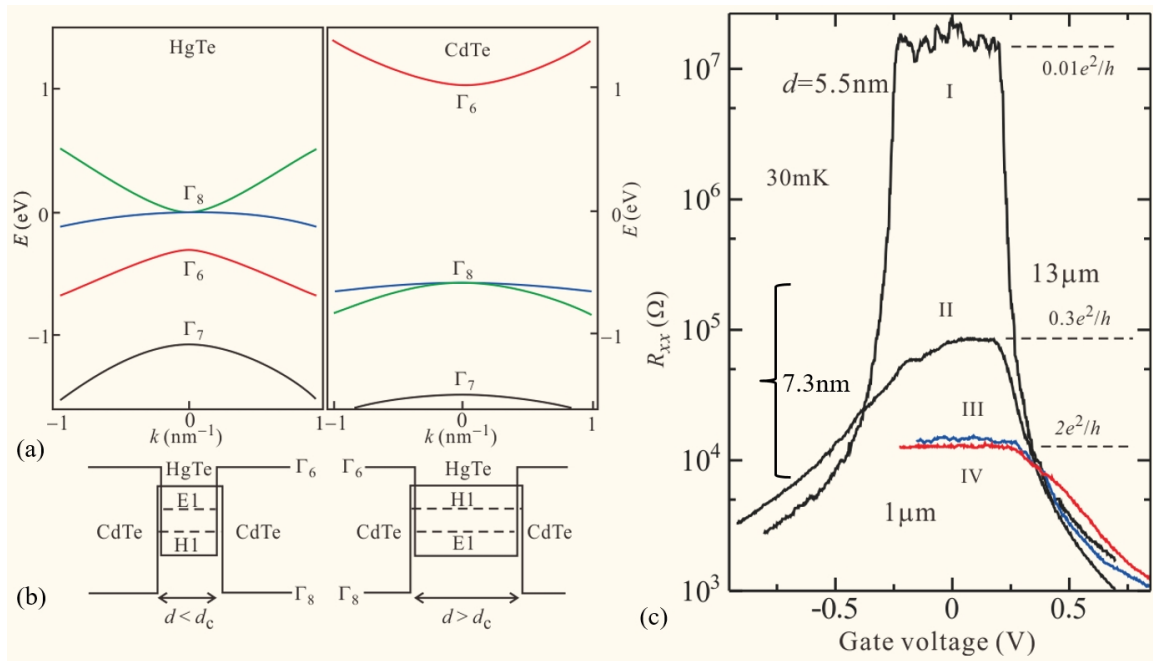


**Fig. 10.8** (a) Band structure around  $\Gamma$ -point of HgTe and CdTe.  $\Gamma_6, \Gamma_7, \Gamma_8$  are Koster symbols for space group elements, which indicate the symmetries of the bands. (b) Schematic view of the positions of E1 and H1 subbands. (c) Longitudinal resistances of CdTe/HgTe/CdTe quantum wells. The gate voltage is measured from the position at which the Fermi level comes to the center of the gap. Well widths, I: 5.5 nm; II, III, IV: 7.3 nm. The distance between the electrodes are  $13 \mu\text{m}$  for I and II,  $1 \mu\text{m}$  for III and IV.

the "quantum spin Hall effect" is that quantum hole insulators, which have a long history, are also considered to be a type of topological insulator, so the first topological insulator discovered by humans is called the quantum hall insulator. The reason why I've added "quantum spin Hall effect" is that quantum Hall insulators, which have a long history, are also considered to be a type of topological insulator, so the first topological insulator discovered by humans should be the quantum Hall insulator and I think we need to mention that clearly.

Figure 10.8 shows the setup of the experiment and the results. HgTe is used as the topological insulator. A thin film of HgTe is inserted between two CdTe films, which work as barrier layers and form a quantum well. Figure 10.8(a) shows the band diagrams of HgTe and CdTe zinc blende crystals calculated by 8-band k-p model with SOI. In CdTe, just like GaAs, the  $\Gamma_6$  ( $J = \pm 1/2$ ) conduction band mainly comes from s-orbital while the  $\Gamma_8$  ( $J = \pm 1/2, \pm 3/2$ ) valence band plus the  $\Gamma_7$  spin-split-off band come from p-orbitals. On the other hand in HgTe, the strong SOI causes a band inversion, that is the  $\Gamma_8$  band floats above the  $\Gamma_6$  band. In a HgTe quantum well, the quantum confinement modifies the band structure. We name quantum-confined level from the electron-like dispersion band  $\Gamma_6$  as E1, and that from the hole-like dispersion band  $\Gamma_8$  as H1.

A theoretical model named Bernevig-Hughes-Zhang(BHZ) model was proposed for the HgTe quantum well[11]. According to the model, as long as the order of E1 and H1 bands on the energy axis keeps the inversion ( $E_{H1} > E_{E1}$ ) the Chern number ( $Z_2$  topological number) is 1 namely the HgTe quantum well is a two-dimensional topological insulator. The quantum well potential is symmetric for the center of well and there is no SIA hence no Rashba SOI. Hence the well structure does not give important change in the SOI. On the other hand, the quantum confinement enhances E1 level and lowers H1 level. With decreasing the well width, then, the order in the level is transformed into the ordinary one at the critical width and the system goes into an ordinary insulator.

In Fig. 10.8(c) the four-terminal resistance of quantum wells of CdTe/HgTe/CdTe, in which the E1-H1 crossing critical width is  $d_c=6.3$  nm. The well widths is 5.5 nm (less than  $d_c$ ) for I and 7.3 nm for others. When the well width is less

than  $d_c$ , the resistance is very high around  $V_g = 0$  indicating that the system is an ordinary insulator. On the other hand when the width is wider than  $d_c$  and H1 level places above E1, a topological insulator is realized and a helical edge state appears at the sample edge. The electric conductance through the helical edge state should be  $2e^2/h$  from the Landauer formula (??). Actually in the samples III (sample width  $1 \mu\text{m}$ ), IV (width  $0.5 \mu\text{m}$ ), the conductances are  $2e^2/h$  around the gate voltage for the insulating phase, which fact indicates the realization of the topological insulating (quantum spin Hall) phase.

## References

- [1] S. Maekawa ed. *Concepts in Spin Electronics*, (Oxford, 2005).
- [2] F. Jedema, A. Filip, B. Van Wees, Nature **410**, 345–348(2001).
- [3] T. Sasaki *et al.*, Applied Physics Express **2**, 053003(2009).
- [4] R. Winkler, *Spin-Orbit Coupling Effects in Two-Dimensional Electron and Hole Systems*, (Springer, 2003).
- [5] G. Dresselhaus, Phys. Rev. **100**, 580–586(1955).
- [6] E. Rashba, Soviet Physics-Solid State **2**, 1109–1122(1960).
- [7] Y. A. Bychkov, E. I. Rashba, Journal of physics C: Solid state physics **17**, 6039(1984).
- [8] A. Därr, J. Kotthaus, T. Ando, Proc. 13th Int. Conf. Phys. Semicond. p.774 (1976) .
- [9] J. Nitta *et al.*, Phys. Rev. Lett. **78**, 1335–1338(1997).
- [10] M. Z. Hasan, C. L. Kane, Rev. Mod. Phys. **82**, 3045–3067(2010).
- [11] A. Bernevig, T. L. Hughes, and S.-C. Zhang, Science **314**, 1757 (2006).
- [12] M. König, S. Wiedmann, C. Brüne, A. Roth, H. Buhmann, L. W. Molenkamp, X.-L. Qi, S.-C. Zhang, Science **318**, 766 (2007).
- [13] S.-Q. Shen, “Topological Insulators” (Springer, 2012).

## Appendix 10A: Motion of small magnetic moment

### 10A.1 Electron spin in a magnetic field

Let us consider a single electron spin  $s$  in static magnetic field  $B_0$  along  $z$ -direction. We consider only the Zeeman energy:

$$\mathcal{H} = (e\hbar/2m_0)gB_0\hat{s}_z = g\mu_B B_0\hat{s}_z,$$

where  $\mu_B$  is the **Bohr magneton**. From the commutatio relatoin of spin operators  $[\hat{s}_j, \hat{s}_k] = i\hat{s}_l/2$  ( $(j, k, l)$  are cyclic replacement of  $(x, y, z)$ ),

$$[\mathcal{H}, \hat{s}_x] = ig\mu_B B_0\hat{s}_y, \quad [\mathcal{H}, \hat{s}_y] = -ig\mu_B B_0\hat{s}_x, \quad [\mathcal{H}, \hat{s}_z] = 0.$$

Hence the Heisenberg equation of motion tells.

$$\frac{\partial \langle s_x \rangle}{\partial t} = -\frac{g\mu_B}{\hbar} B_0 \langle s_y \rangle, \quad \frac{\partial \langle s_y \rangle}{\partial t} = \frac{g\mu_B}{\hbar} B_0 \langle s_x \rangle, \quad \frac{\partial \langle s_z \rangle}{\partial t} = 0. \quad (10A.1)$$

$$\therefore \langle s_x \rangle = A \cos \omega_0 t, \quad \langle s_y \rangle = A \sin \omega_0 t, \quad \langle s_z \rangle = C, \quad \omega_0 = \frac{eg}{2m_0} B_0, \quad (10A.2)$$

where  $A^2 + C^2 = s^2$ . Equation (10A.2) is representing precession around  $z$ -axis with the **Larmor frequency**  $\omega_0$ .

Next we add a rotating magnetic field  $B_1(e_x \cos \omega t + e_y \sin \omega t)$  in  $xy$ -plane. The time-dependent Hamiltonian with that is written as

$$\mathcal{H}(t) = g\mu_B (B_1 \cos \omega t \hat{s}_x + B_1 \sin \omega t \hat{s}_y + B_0 \hat{s}_z).$$

The time evolution of spin-wavefunction  $\chi(t) = u(t)|\uparrow\rangle + d(t)|\downarrow\rangle$  is represented as

$$i\hbar \frac{\partial}{\partial t} \begin{pmatrix} u \\ d \end{pmatrix} = -g\mu_B \begin{pmatrix} B_0 & B_1 e^{-i\omega t} \\ B_1 e^{i\omega t} & -B_0 \end{pmatrix} \begin{pmatrix} u \\ d \end{pmatrix}.$$

The solutions of the above simultaneous differential equations are expressed as

$$u(t) = C(\Omega \mp \omega_0 \pm \omega) e^{i(\pm\Omega - \omega)t/2}, \quad (10A.3a)$$

$$v(t) = \pm C\omega_c e^{i(\pm\Omega + \omega)t/2}, \quad (10A.3b)$$

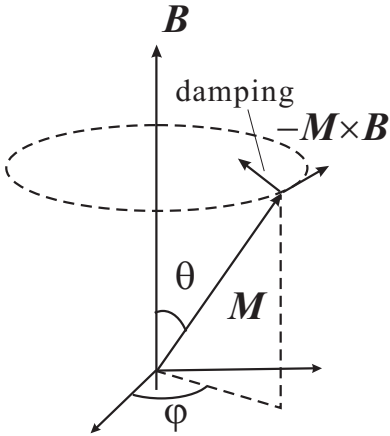
where  $C$  is an integration constant,  $\omega_c = eB_1/m_0$ , and  $\Omega = \sqrt{(\omega - \omega_0)^2 + \omega_c^2}$ . Taking the initial condition as  $u(t) = 1$ ,  $d(t) = 0$ , the solutions are

$$u(t) = \sqrt{2 - \frac{\omega_c^2}{\Omega^2}} \sin\left(\frac{\Omega t}{2} + \alpha\right) e^{-i\omega t/2}, \quad v(t) = \frac{\omega_c}{\Omega} \sin\frac{\Omega t}{2} e^{i\omega t/2},$$

where  $\alpha = \arctan(\Omega/(\omega - \omega_0))$ . Then we obtain

$$|d(t)|^2 = \frac{\omega_c^2}{(\omega - \omega_0)^2 + \omega_c^2} \sin^2 \frac{\Omega t}{2}, \quad (10A.4)$$

which indicates a Lorentz type resonance and the oscillation with the frequency  $\Omega (= \omega_c)$  at  $\omega = \omega_0$ .



## 10A.2 LLG equation

Applying the equation of motion (10A.1) to a general macroscopic magnetic moment  $M$ , we obtain the Landau-Lifshitz equation

$$\frac{\partial M}{\partial t} = -\frac{g\mu_B}{\hbar} M \times B. \quad (10A.5)$$

The addition of the relaxation  $\mathcal{R}$  of  $M$  gives

$$\frac{\partial M}{\partial t} = -\frac{g\mu_B}{\hbar} M \times B + \mathcal{R}. \quad (10A.6)$$

What should be the mathematical form of  $\mathcal{R}$ ? Since  $M$  has the lowest energy at the direction of  $B$ , the relaxation should be a force to this direction as shown in the left. The force is perpendicular to  $-M \times B$  and  $M$ . It is natural to infer that

$$\mathcal{R}_{LL} = -\lambda \frac{M}{|M|} \times (M \times B), \quad (10A.7)$$

where  $\lambda$  is a constant. This is called the Landau-Lifshitz damping term.

Another idea is that the relaxation rate should be proportional to time-variation of  $\partial M/\partial t$ , which has the same direction as  $-M \times B$ . In this idea the damping term can be written with a constant  $\alpha$  as

$$\mathcal{R}_G = \alpha \frac{M}{|M|} \times \frac{\partial M}{\partial t}, \quad (10A.8)$$

which is called Gilbert damping term. If we substitute the equation of motion (10A.5) into this  $\partial M/\partial t$ , the term is the same as the Landau-Lifshitz term. Adopting  $\mathcal{R}_G$  for the damping, we reach the **Landau-Lifshitz-Gilbert (LLG)** equation:

$$\frac{\partial M}{\partial t} = -\frac{g\mu_B}{\hbar} M \times B + \alpha \frac{M}{|M|} \times \frac{\partial M}{\partial t}, \quad (10A.9)$$

which is often used to describe motions of magnetization phenomenologically.